BULLETIN OF THE POLISH ACADEMY OF SCIENCES
TECHNICAL SCIENCES, Vol. 63, No. 1, 2015
DOI: 10.1515/bpasts-2015-0007

Analysis of the microcracking process with the Acoustic Emission method with respect to the service life of reinforced concrete structures with the example of the RC beams

B. GOSZCZYŃSKA* , G. ŚWIT, and W. TRĄMPCZYŃSKI

Faculty of Civil Engineering and Architecture, Kielce University of Technology,
7 Tysiąclecia Państwa Polskiego Ave., 25-314 Kielce, Poland

Abstract. The study presents the analysis of the process of crack formation and crack width growth in statically determinate and hyperstatic reinforced concrete beams with the IADP acoustic emission method. The beams were subjected to the monotonic, variable with unloading, and variable cyclic loading schemes. The criteria of structural damage were established to account for the structure durability.

Key words: service life, destructive process, acoustic emission, 3D scanner Aramis.

1. Introduction

Durability of building and engineering structures has been a subject of growing importance in recent years. That refers both to the stage of integrated design [1], and in particular, to the maintenance stage. The latter is often related to the necessity of extending the lifespan of the existing structures or changing their use. As regards the design stage, the durability is accounted for in the Basis of structural design PN-EN 1990, which defines the design service life of the structure as a period in which the structure or its part is to be used as intended, with proper maintenance, and is not in need of major repairs. In the Model Code 2010, the design service life was additionally related to the suitability criteria and the required reliability level. It is very difficult to assess the durability of existing structures, understood as the remnant non-failure time of service, when the actual loading, structure condition, and environmental impacts are to be accounted for. The assessment of structural reliability, carried out on the basis of detailed analysis, bears a certain probability. At the maintenance stage, it is also important to predict how long a given structure will be capable of delivering reliable performance, which greatly affects the assessment probability level. Because the probability level of the durability assessment is not always satisfactory, it is increasingly frequently recommended to monitor the structure condition, which most often refers to bridges. The necessity to guarantee structural reliability produces the recommendation, stipulated by law, for monitoring the structure performance in service on current basis. Properly conducted routine inspections, based on the objective results of monitoring and diagnostics, make it possible to extend the structure lifespan and to select the optimum time and scope of rehabilitation, repairs or upgrading. When faults are found that pose a threat to the structural reliability, inspections help to make a decision on putting a structure out of service. Non-destructive testing (NDT) methods [2, 3], which have been rapidly developing over recent years, provide objective means to collect information on the strength of materials and its variation in time. NDT also makes it possible to evaluate other features, such as component dimensions, location of faults, damages and microcracks, that of reinforcement, and also a degree of corrosion hazard. The method based on the measurement and analysis of acoustic emission (AE) signals generated by active destructive processes caused by the loading action in the examined member, or in the whole structure, could be most obviously classified as NDT. The analysis of identification and location of destructive processes provides a basis for the diagnostics of the examined structures [4–14]. The obvious advantage offered by the method is the possibility of conducting measurements of the whole structure of concern (e.g. bridge), or of its part [11].

The durability of reinforced concrete structures is a derivative of microcracking of concrete, which is to protect reinforcement against corrosion throughout the whole of the structure life [15]. Caused by volumetric changes in the cement grout, internal stresses occur in concrete members almost from the very beginning of their moulding. That results in microcrack formation in the grout or at the cement grout – aggregate grain or rebar interface. Because of external factors (e.g. a load) acting on the structural member, microcracks can change their width, length, and they can coalesce forming crack nuclei on the member surface. Cracks are inherent in concrete members and are not decisive for the load-bearing capacity over a short period of time. Consequently, limiting crack widths is intended to prevent corrosion attack which shortens the life of the structure and lower its aesthetics. Research methods that are employed to assess structural health and durability of reinforced concrete structures need to account for a multitude of factors that affect cracking, non-homogeneity of materials, and a complex pattern of stress and strain that accompany crack initiation and growth [16].

*e-mail: b.goszczynska@tu.kielce.pl

The study presents the analysis of the process of crack initiation and their width growth in statically determinate and hyperstatic reinforced concrete beams with the IADP (Identification of Active Damage Processes) acoustic emission method. The beams were subjected to monotonic, variable with unloading and cyclic modes of loading. The criteria of structural damage, taking into account the structure durability, were developed.

2. Basics of the IADP acoustic emission method and experimental procedure

The acoustic emission (AE) method IADP relies on the analysis of acoustic waves generated by active destructive processes that develop in building and engineering structures under service load. AE signals are received by acoustic sensors spaced over the structure, covering the whole of its volume, and then compared with the reference signal database, which is presented in the form of a diagram in Fig. 1.

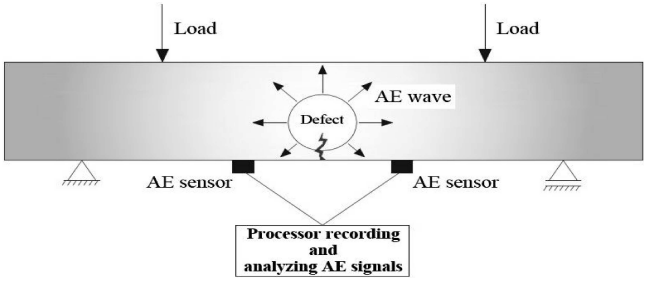

Fig. 1. Diagram of wave generation by destructive processes and wave recording

The reference database was complied before for specific destructive processes on the basis of twelve acoustic wave parameters: the number of counts, number of counts to peak amplitude, signal duration, signal rise time, signal amplitude, signal energy, signal strength, signal mean effective voltage, signal absolute energy, signal mean frequency, reverberation frequency, and signal initiation frequency. The means of compiling the reference signal database is presented in [9, 13].

Destructive processes, identified on the basis of a comparative analysis, are then located by analysing differences in the AE signal arrival time at individual sensors. Zone or linear location is used in the procedure. The AE method offers a clear advantage in making it possible to space sensors recording AE waves in such a way that the whole structure is covered by measurements. Another benefit brought by the method is the possibility of conducting tests under actual service load.

The method (named as RPD – Recognition of Destructive Processes) was formerly developed for reinforced concrete structures [5, 9, 11, 13] and the following destructive processes were defined for the reference data base: microcracking in the concrete at the interface of the small-sized ($\Phi \leq 2$ mm) aggregate fraction and the cement mortar, microcracking in the concrete at the interface of the small-sized and medium-sized ($\Phi \leq 8$ mm) aggregate fraction, crack initiation in the concrete tension zone, cracking at the concrete-reinforcement interface crack development, plastic deformation of steel and concrete friction, concrete delamination, rupture of prestressed tendons.

The validation of the method using the 3D scanner Aramis system confirms it is possible to identify destructive processes, related mainly to crack initiation and growth under loading, in reinforced concrete members [10, 14].

The processes that generate AE signals accompany only active damages, i.e. those arising, or developing under the conditions that prevail at the time measurements are carried out. The defects present in the structure, which are not in the development stage, do not generate AE signals. Thus, the method can be employed to estimate the effectiveness of renovation or upgrading.

The investigations conducted confirmed that the concept of the RPD acoustic emission method could be applied to the testing of reinforced concrete structures [13, 14].

As crack formation is not allowed in the pre-stressed structures in most cases, whereas in reinforced concrete structures, cracks are inherent and permissible within certain width limits, it was necessary to modify classes of destructive processes. Hence, the name of method was altered and the IADP (Identification of Active Damage Processes) name was proposed. The classes adopted in the reference signal database for reinforced concrete structures [14] are as follows:

Class 1 Initiation of cracking in the grout;

Class 2 Initiation of cracking at the grout-aggregate interface;

Class 3 Initiation of micro-cracks;

Class 4 Growth of cracks;

Class 5 Loss of adhesion in the crack vicinity;

Class 6 Buckling of compression bars;

Class 7 Crushing of compression concrete;

Class 8 Rebar rupture.

Mean values of AE signal parameters for signal Classes 3, 4 and 5 are presented in Table 1.

Table 1
Mean values of AE signals parameters for the reference database

Reference database Class No	3	4	5
Mean values of AE signals			
Signal rise time [μs]	276.8	258.18	294.49
Number of counts to peak amplitude	6.92	6.67	9.33
Number of counts	947.6	5300.8	7561.5
Signal energy [1 μVs/counts]	887.0	4260	7948
Signal amplitude [dB]	72.76	77.21	83.01
Signal mean frequency [kHz]	20.01	23.70	30.40
Signal mean effective voltage [V]	0.33	0.42	0.71
Reverbation frequency [kHz]	19.93	71.57	30.39
Signal initiation frequency [kHz]	101.3	71.57	47.3
Signal absolute energy [aJ]	5.5e+5	2.0e+6	6.7e+6
Signal strength [pVs]	5.5e+6	2.6e+7	5.0e+7
Signal duration EA [μs]	47396	220322	248140

Tests carried out on statically determinate and indeterminate beams demonstrate that Classes 6, 7 and 8 occur just before failure, and almost simultaneously. The signals of those

final classes could be joined to form a single Class 6, which will summarize failure patterns caused by the following: concrete crushing, bar buckling and rebar rupture. Hence, for reinforced concrete structure, the reference signal database comprises six classes of AE signals. Graphic symbols to represent individual classes are presented in Table 2.

Table 2
Graphic denotation of AE signal classes

Class no.	1	2	3	4	5	6
Denotation of AE signal classes						

AE signals identified as belonging to:

Class 3 Initiation of micro-cracks

Class 4 Growth of cracks

Class 5 Loss of adhesion in the crack vicinity

accompany crack formation and growth in the reinforced concrete member. As the crack advancement significantly affects the structure service life, the criteria of structural damage were established, using the IADP acoustic emission method, on the basis of the analysis of the classes of destructive processes mentioned above.

Tests conducted for reinforced concrete beams using Aramis optical 3D scanner [10, 14, 17] show the IADP acoustic emission method makes it possible to identify and locate Class 3 and 4 signals. Those correspond to crack initiation and growth, so it is possible to detect the development of load-induced cracks. Also, cracks resulting from dominant bending and shear loads can be differentiated [14].

The theory of continual changes in stiffness, formulated by Kuczyński [18] and Goszczyński [19], was based on the analysis of experimental results derived from large-scale tests on reinforced concrete beams. At the core of the theory lies an observation that the phenomena accompanying concrete performance, i.e. plastification and cracking, inherently discontinuous, when referred to average values of result sets, can be described with continuous and monotonic functions. Properties of materials can be interpreted in a similar way. Fibre, extracted from a concrete member, has much diversified structure, it contains solid, liquid and gaseous phases, which have different mechanical properties. The fibre structure is discontinuous, and discontinuity areas are randomly distributed (Fig. 2).

Fig. 2. Exemplary structure of the fibre extracted from concrete

Due to a chaotic distribution of concrete ingredients, a cross-section through a few fibres also covers different phases. Thus, it can be said that a concrete cross-section, understood as an infinitely thin body sample is, concurrently, a solid, liquid and gaseous material. To put it in other words, such cross-section shows the properties of solid, liquid and gaseous body at the same time.

Such an interpretation, assumed for the sake of many analyses, results in an assumption on the material continuity, and in ascribing averaged concrete properties to each point of the section. Understood as indefinitely small segment (elementary segment) $dV = dx, dy, dz$, each section point can be a solid material with the probability of Ps, liquid material with the probability of Pc, or gaseous material with the probability of Pg. It can also be stated that over time, the quantities representing those probabilities, thus properties, will undergo changes. The advancing process of cement hydration increases the probability of solid phase occurrence at the expense of others. The grout shrinkage itself results in stress occurrence, which leads to the formation of microcracks and even macrocracks, thus the probability of the gaseous phase grows. The same effect is produced by loading. Ambient thermal and humidity conditions affect the probability of occurrence of the liquid and gaseous phases. Therefore, it can be said that concrete properties largely depend on the probabilities of occurrence of individual phases, which is clearly reflected in the process of crack initiation and growth. Concrete, and grout in particular, have complex chemical structure. Neither solid nor liquid phase is homogenous. The diversity in structure results in the fact that individual elementary segments, even within the same phase, have different mechanical properties which affect the advancement of cracking.

Adopting such an approach, the width analysis of cracks corresponding to defined Classes of destructive processes, based on numerous test results for reinforced concrete beams, was carried out for mean values of moments/loads generating AE signals ascribed to those classes.

3. Experimental testing

3.1. Test objects. Tests were conducted for 40 reinforced concrete beams, plant-precast from C40/50 concrete and B500SP class reinforcement steel. Out of those, 26 items were used to conduct tests for single-span simply supported beams. The remaining 14 items were used for tests on double-span beams. Single-span beams having 120×300 mm cross section and 3000 mm length, between the support, differed in the structure of longitudinal and transverse reinforcement. They were also subjected to different loading schemes, namely sixteen were loaded until failure due to the bending moment, and ten due to the action of the shear force.

In the case of single-span beams, dedicated to bending, two ratios of longitudinal reinforcement were applied $\rho_l = 0.7\%$ (2∅12) and $\rho_l = 2.0\%$ (3∅12+2∅14) with stirrups ∅6 spaced every 10 cm between support and applied force, and every 21.5 cm between acting forces (excluding the four beams without stirrups between acting forces). In the case of the beams devoted to shearing, the longitudinal reinforcement was 3∅12 + 2∅14 ($\rho_l = 2.0\%$) and degree of web reinforcement was diminished to ρ_w minimum.

For the sake of comparative analysis, double-span beam dimensions were the same as those of single-span ones, i.e. 120×300 mm cross section and 3000 mm length between the single support. The reinforcement of a double-span beam

was composed of six ∅12 bars arranged in two arrays. In the first one, two bars are located in upper fibres of the beam, and four in the bottom fibres (six beams). The other array featured three bars placed in the upper fibres of the beam, and located symmetrically to those, the remaining three in the bottom fibres (six beams). In two beams, the transverse reinforcement was reduced to the minimum to enforce shear failure. Exemplary scheme of the reinforcement structure in the single-span beam is presented in Fig. 3, and that of double-span beam – in Fig. 4.

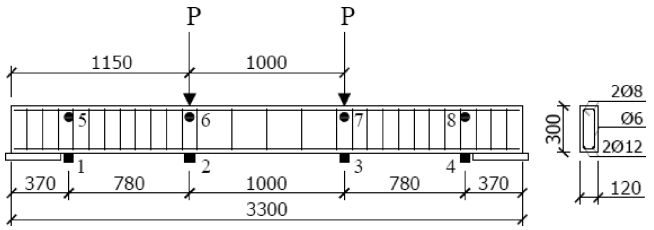

Fig. 3. Diagram of the bending test and the scheme of reinforcement structure for a single-span beam with AE sensor spacing

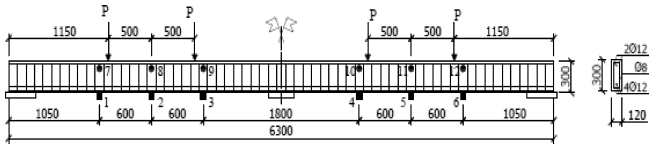

Fig. 4. Diagram of the bending test and the scheme of reinforcement structure for a double-span beam with AE sensor spacing

3.2. The experimental setup and the equipment. Tests were conducted at the experimental setup at which single- and double-span beams were loaded, using actuators with a controller, in accordance with the loading scheme. The equipment installed on the setup allowed making comparative analyses of the experimental results. The equipment consisted of the following items:

1. ARAMIS optical 3D scanner – used to record strains within the beam surface (field strain) in loading.
2. Hottinger Baldwin Messtechnik measurement system – to measure displacements as a function of load, five induction sensors were used.
3. acoustic emission measurement system – to record and analyse acoustic emission signals in the loading process.

The experimental setup with the reinforced concrete double-span beam fixed at it, ready for the experiment, together with the measurement equipment is shown in Fig. 5.

The equipment was synchronised with the pre-programmed load. As the beam was loaded, the data from the equipment were recorded. The data included the following: values of the loading forces, displacements recorded by five induction sensors, acoustic emission signals and strain within the beam surface. In this way it was possible to identify, locate and validate the recorded acoustic emission signals with respect to observed destructive processes that occur in reinforced concrete members under loading, particularly the process of crack initiation and growth.

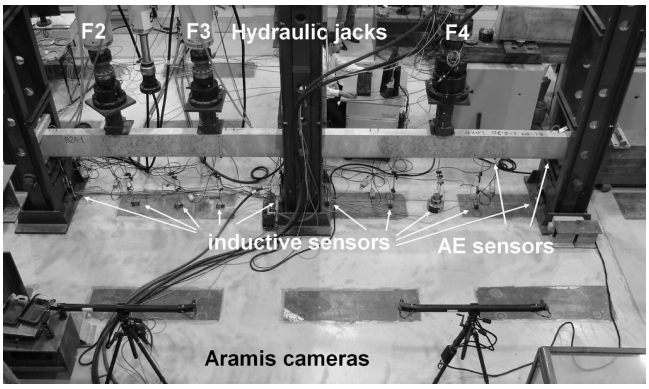

Fig. 5. Reinforced concrete beam at the experimental setup with individually controlled actuators, AE sensors, displacement sensors, and Aramis 3D scanner

3.3. Test programme and execution. In the tests, conducted until failure, acoustic emission signals, generated by load-induced destructive processes, were recorded using the processor and AE sensors. At the same time, beam vertical displacements were measured using induction sensors and the 60-channel *Hottinger* measurement system. The non-standard arrangement of the Aramis system [17] made it possible to measure strains within pre-prepared lateral surfaces of the beams. The system allows tracing crack initiation and growth, including crack width increase, which is associated with the local strain concentration. That can be done continuously at all load levels.

Acoustic emission (AE) tests were conducted using 24-channel *PhysicalAcousticCorporation* measurement system. The system comprises three PCI-8 processors, with filters on the measurement channels, and with applications for signal recording and analysis available through the *AEwin* control panel. Measurements were taken using SE 55-R sensors with 1220 type, 40 dB gain, pre-amplifiers. Recorded acoustic emission signals were subjected to statistical analysis using NOESIS software, which is based on the image recognition method.

Bending (16 beams) and shear (10 beams) tests were performed for single-span beams in accordance with three loading schemes:

M – monotonic loading, until failure, with two identical forces

O – loading with two identical forces, with unloading, at five load levels determined depending on the load-bearing capacity of the beams

C – low-cycling load, at two or three load levels, sinusoidal – to simulate a driving vehicle.

The cyclic load program was taken as a simulation of the operating load caused by passing vehicles according to the durability tests of the bituminous pavements [20].

A diagram of the bending test for a single-span beam, together with a spacing array of AE sensors (1-8) is presented in Fig. 3. The sites of pre-prepared beam surfaces for the field strain test are shown in Fig. 6. The Aramis system was used in the test, for the beams intended to fail due to the bending

moment (Fig. 6a), one arm with two digital video cameras was employed. Two arms, each equipped with two cameras, were used when the beam failure was to be caused by a shear force (Fig. 6b).

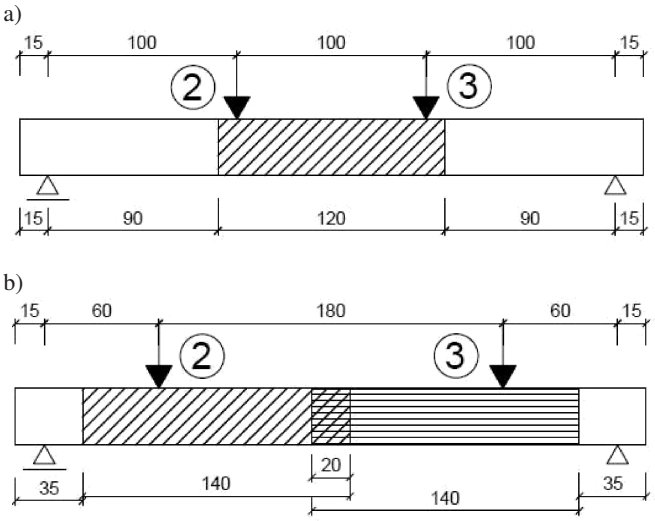

Fig. 6. a) Bending load and area examined with Aramis (one arm), b) shearing load and area examined with Aramis (two arms)

Twelve double-span beams (Fig. 4) were subjected to variable bending load until failure in accordance with three loading schemes A, B and C:

A – Loading scheme that resulted in the failure of the span loaded with one concentrated force. The scheme, together with the diagram of support, and of surfaces where field strain measurements were taken using the Aramis system is shown in Fig. 7.

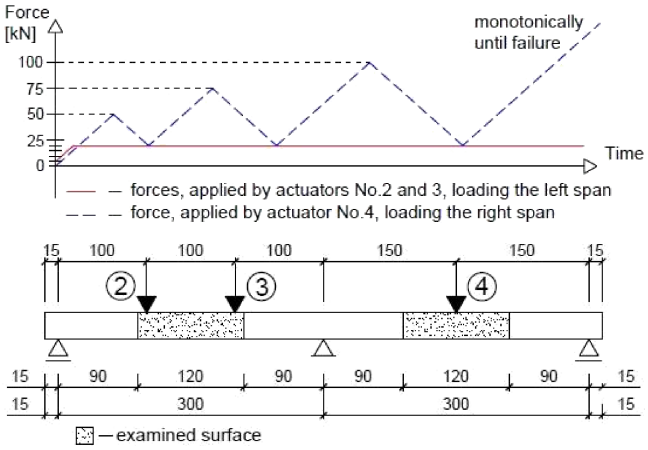

Fig. 7. Variable loading scheme (A) and areas examined with 3D scanner Aramis

B – Loading scheme that resulted in the failure of the span loaded with two forces. The scheme, together with the diagram of support, and of surfaces where strain measurements were taken using the Aramis system is presented in Fig. 8.

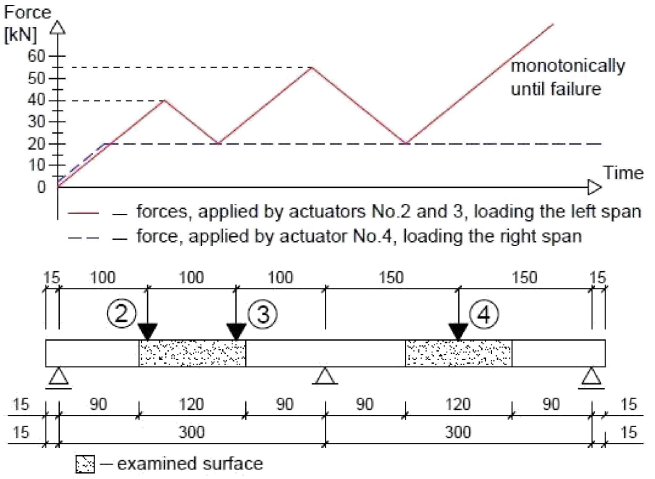

Fig. 8. Variable loading scheme (B) and areas examined with 3D scanner Aramis

C – Loading scheme that involved variable cyclic load. The scheme, together with the diagram of support, and of surfaces where strain measurements were taken using the Aramis system can be seen in Fig. 9.

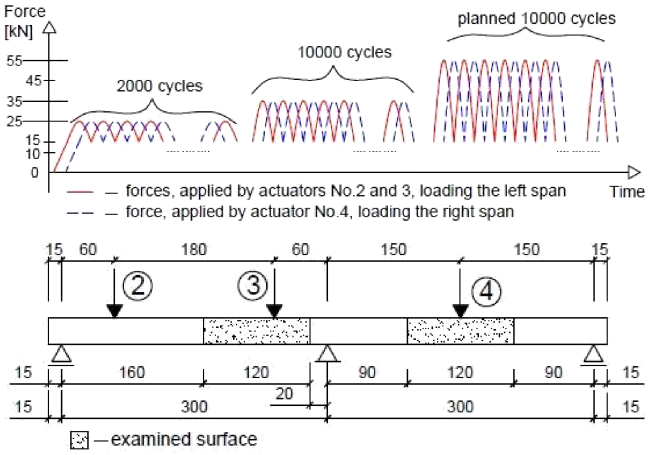

Fig. 9. Cyclic loading scheme (C) and areas examined with 3D scanner Aramis

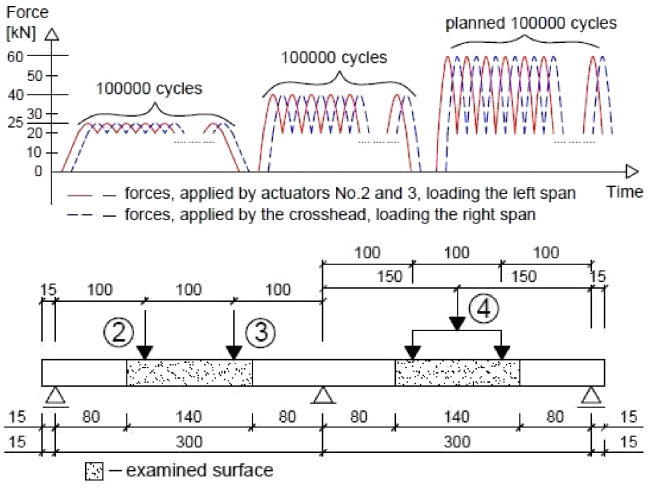

Fig. 10. Variable cyclic loading scheme causing shear failure with areas examined with 3D scanner Aramis

Two beams, in which transverse reinforcement was reduced to the minimum to obtain shear failure, were loaded as shown in Fig. 10.

The array of acoustic emission sensors (1-12) for double-span beams loaded until bending failure in accordance with A and B loading schemes are shown in Fig. 4.

4. Analysis of results

The results of simultaneous recording of AE signals (AE measurement system) and of strains within the beam surface (Aramis system), obtained in tests run for 40 beams, made it possible to analyse crack widths accompanying acoustic emission signals ascribed to Class 3, 4 and 5.

Table 3
Moments/values of loading forces corresponding to the formation of Class 3, 4 and 5

Monotonic load										
Beam	Mean Load	Calsses 3		4		5		Relative load for classes [%]		
	[kN]	Time [s]	Force [kN]	Time [s]	Force [kN]	Time [s]	Force [kN]	3	4	5
A1M-1	**34.38**	583	**12.90**	917	**15.17**	1458	**18.19**	**37.5**	**44.1**	**52.9**
A1M-2	**35.75**	488	**8.96**	854	**10.71**	1610	**15.17**	**25.1**	**30.0**	**42.4**
A2M-1	**81.98**	54	**3.10**	1304	**9.62**	3566	**25.02**	**3.8**	**11.7**	**30.5**
A2M-2	**78.85**	1605	**13.50**	2200	**17.82**	4798	**35.64**	**17.1**	**22.6**	**45.2**
C2M-1	**88.02**	930	**9.09**	1919	**15.67**	2674	**21.01**	**10.3**	**17.8**	**23.9**
C2M-2	**84.12**	280	**4.94**	1568	**13.62**	3570	**27.38**	**5.9**	**16.2**	**32.5**
D2M-1	**87.22**	630	**7.30**	2885	**22.77**	6857	**49.67**	**8.4**	**26.1**	**57.0**
D2M-2	**81.27**	597	**7.09**	1005	**9.96**	1955	**16.63**	**8.7**	**12.3**	**20.5**
							Mean relative force	**14.60**	**22.60**	**38.11**
							Standard deviation	**11.50**	**10.82**	**13.34**
							Coeficient of variation	**78.8%**	**47.9%**	**35.0%**

Table 4
Crack widths corresponding to Class 3, 4 and 5 – bending failure

Beam	Class	Denotation of AE signal classes	Relative loads for classes [%]	Absolute loads [kN]	Maximum width crack [mm]	Mean width crack [mm]
A1M-2	3		14.79	5.56	0.05	0.01
	4		22.82	8.58	0.10	0.06
	5		39.08	14.69	0.18	0.11
A2M-1	3		14.79	12.25	0.07	0.01
	4		22.82	18.91	0.07	0.02
	5		39.08	32.38	0.12	0.04
A2M-2	3		14.79	11.69	0.09	0.02
	4		22.82	18.04	0.08	0.03
	5		39.08	30.88	0.13	0.06
C2M-1	3		14.79	13.13	0.10	0.03
	4		22.82	20.27	0.10	0.04
	5		39.08	34.71	0.16	0.08
C2M-2	3		14.79	12.57	0.06	0.03
	4		22.82	19.41	0.15	0.05
	5		39.08	33.23	0.22	0.10
D2M-1	**3**		14.79	12.98	0.04	0.01
	4		22.82	20.04	0.07	0.02
	5		39.08	34.31	0.13	0.06
D2M-2	**3**		14.79	12.18	0.03	0.01
	4		22.82	18.80	0.08	0.03
	5		39.08	32.19	0.13	0.06

First, on the basis of the parameter summation diagrams, the strength of AE signals was determined as a function of the load applied. That was done for individual beams and measurement bases (beam fragments between AE sensors). Also, the values of moments corresponding to the recording of destructive processes categorised as Class 3, 4 and 5 were determined. For double-span beams, moments were computed for both spans and at the support. For the purpose of a cumulative analysis, relative moments were calculated as the ratio of the value of a moment for which Class 3, 4 and 5 signals, respectively, were recorded to the moment equal the load-bearing capacity of reinforced concrete cross-section in the analysed measurement base.

Exemplary results of computations performed for single-span beams loaded monotonically until bending failure, where the moment is equal to the load, are presented in Table 3. Crack widths corresponding to Class 3, 4 and 5 are presented in Table 4.

As regards double-span beams, the computed values of relative moments corresponding to the occurrence, in the spans and at the support, of the classes of destructive processes of concern, are presented in Figs. 11, 12 for Class 3 and 4 respectively.

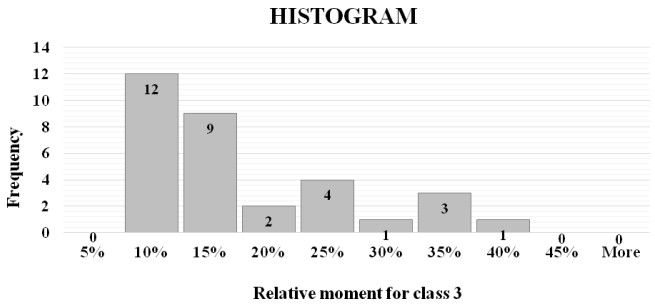

Fig. 11. Histogram of the relative moment corresponding to Class 3 formation

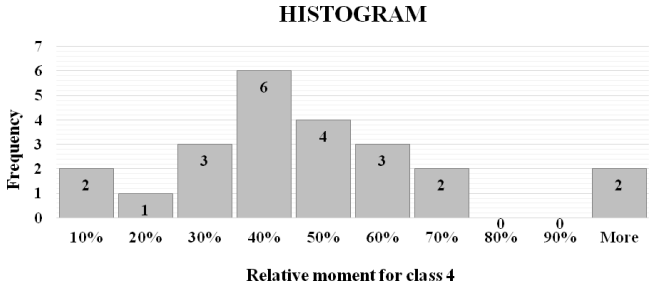

Fig. 12. Histogram of the relative moment corresponding to Class 4 formation

Cracks widths corresponding to Class 3, 4 and 5 were determined in the same way as for single-span beams taking into account both the left and right span.

It is observed that both for single-span and double-span beams, the scatter of results for loads/relative moments corresponding to the occurrence of classes of destructive processes, is high as expected. On the other hand, the number of experimental results is also large.

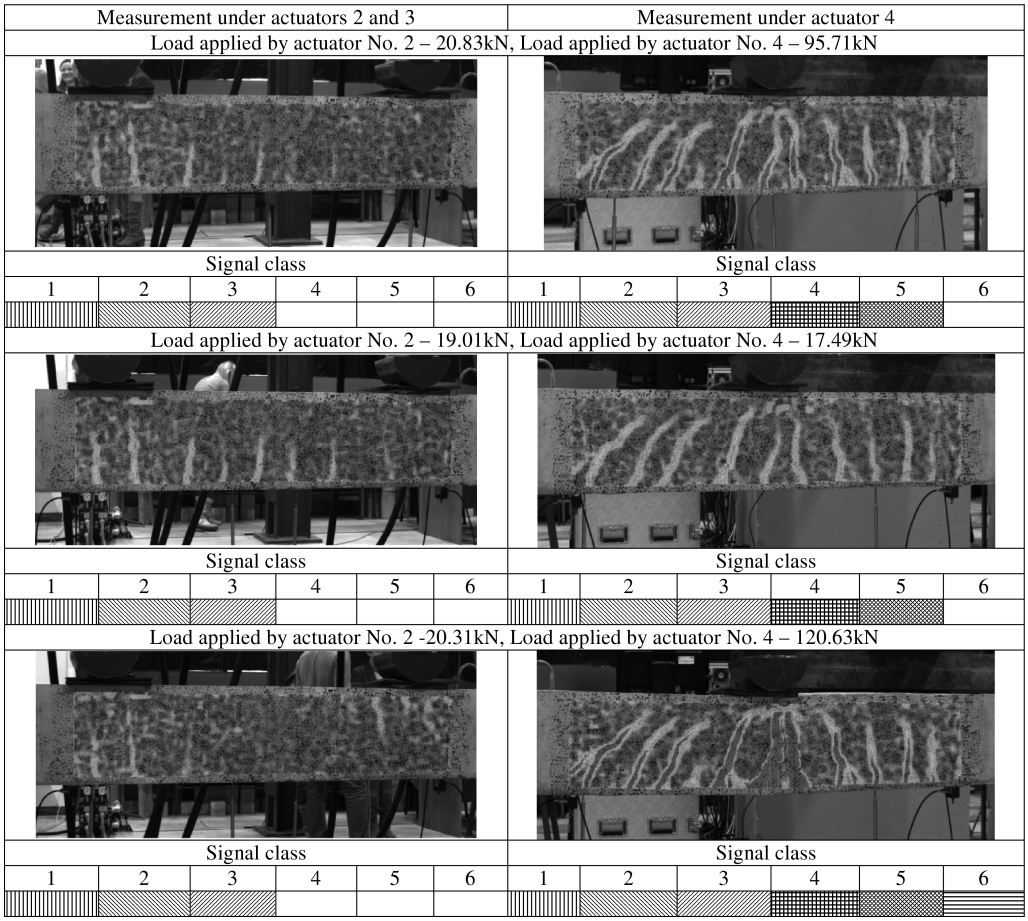

Fig. 13. Exemplary image of crack advancement with identified classes of destructive processes at three levels of the double-span beam loading (an exemplary double-span beam loaded according to the scheme A)

The tests conducted for the study on both single- and double-span reinforced concrete beams, using synchronised testing equipment (actuators, AE measurement system – Aramis optical scanner), made it possible to trace the process of initiation and width growth of cracks corresponding to specific classes of destructive processes. The graphic representation of the cracking process tracing is given in Fig. 13 for an exemplary double-span beam loaded according to the scheme (A) – until failure with one concentrated force.

The left hand side of the figure shows the cracking of the span loaded by two forces (actuators 2 and 3), whereas the right hand side illustrates the span loaded with one force (actuator 4). That is done for three successive loading levels with classes of identified destructive processes denoted in the way presented in Table 2. The loading scheme, together with the areas examined with the Aramis system, is presented in Fig. 7.

For reinforced concrete structures, conclusions regarding the advancement of cracking should not be based on the results of a single test. Taking that into account, all results of experimental beam tests were considered to assess a degree of damage to a structural member. On the basis of the results, the maximum and average crack widths were determined at the height of the centre of gravity of the reinforcement in tension. The cracks resulted from the action of the computed mean relative (to the load-bearing capacity) loads that cause the generation of acoustic emission signals identified as Class 3, 4 and 5.

On the basis of the experimental results for all 40 beams with different loading history, it can be stated that:

- **for single-span beams under different loading schemes (monotonic, with unloading, and cyclic)**
  1. The maximum crack widths computed in central parts (constant bending moment) of beams subjected to a bending load are as follows: for Class 3 – 0.1 mm; Class 4 – 0.15 mm, and Clas 5 – 0.22 mm, which confirms that classes are related to crack development.
  2. The maximum crack widths computed for the left and right hand side of the beams subjected to a shearing load are as follows: on the beam right hand side, for Class 3 – 0.08 mm, for Class 4 – 0.06 mm, and for Class 5 – 0.17 mm, on the beam right hand side, for Class 3 – 0.08 mm, for Class 4 – 0.07 mm, and for Class 5 – 0.15 mm. The maximum crack widths obtained on both sides of the beam show very close values, which indicates the reliability of the analysis. It can be observed that the maximum crack width

virtually does not change for Class 3 and 4, whereas crack development occurs only in Class 5. That results from the fact that the crack width was computed at the height of the centre of gravity of the reinforcement in tension, and with a high amount of transverse forces, skew cracks are formed closer to the beam midspan.

- **for double-span beams under different loading schemes (variable load: A and B, cyclic load: C)**

  1. The maximum crack widths computed for the parts of beams covered with scanning, loaded in accordance with scheme A, are as follows: for Class 3 – 0.07 mm; Class 4 – 0.15 mm, and Class 5 – 0.20 mm.
  2. The maximum crack widths computed for the parts of beams covered with scanning, loaded in accordance with scheme B, are as follows: for Class 3 – 0.05 mm; Class 4 – 0.17 mm, and Class 5 – 0.27 mm.
  3. The maximum crack widths computed for the parts of beams covered with scanning, loaded in accordance with scheme C, are as follows: for Class 3 – 0.04 mm; Class 4 – 0.12 mm, and Class 5 – 0.18 mm.

The scatter of results, found on the basis of standard deviation and variation coefficient, can be explained by a strongly random character of crack formation in reinforced concrete members. Therefore, when criteria of the degree of structural damage are established, high scatter of results must be considered.

5. Conclusions

1. Taking into account the maximum widths of cracks generating acoustic emission signals of Class 3, 4 and 5, and also the graphic cracking image obtained with the scanner, it can be concluded that the criteria of structural damage can be applied both to statically determinate members (single-span beams) and to statically indeterminate members (double-span beams).
2. On the basis of the analysis of crack development, accompanied by acoustic signals of Class 3, 4 and 5, and the corresponding crack widths, the following criteria were adopted for the sake of assessment of the condition of reinforced concrete structures:
   Class 1 and 2 – safe performance
   Class 3 – warning
   Class 4 – threat to durability
   Class 5 – threat to load-bearing capacity
   Class 6 – loss of structural reliability
   Criteria of structural damage assumed for Class 4 and 5 are justified by a high scatter of results and an increase trend seen in crack width when a member is subjected to cyclic load at the same load value level. That was observed on the basis of crack width analysis for variable loads (with unloading, and low-cyclic ones). Another reason was a decrease in the load-bearing capacity of double-span beams subjected to cyclic loading.
3. The tests carried out for the study confirm that the IADP acoustic emission method can be applied to the analysis of crack formation and advancement in reinforced concrete beams, performed to evaluate a degree of structural damage and to predict the remnant life of the structure.

Acknowledgements. Research was executed under Programme *Innovative Means and Effective Methods of Improvements in Structural Reliability and Durability of Building Structures and Transport Infrastructure in the Sustainable Development Strategy*, subject 6.3.

REFERENCES

[1] A. Ajdukiewicz, "Some aspects of durability and impact on the environment in concrete structures design", *Building Review* 2, 20–28 (2011), (in Polish).
[2] J. Hoła and K. Schabowicz, "State-of-the-art non-destructive methods for diagnostics testing of building structures – anticipated development trends", *Archives of Civil and Mechanical Engineering* 10 (3), 5–18 (2010).
[3] K. Ono, "Application of acoustic emission for structure diagnosis", *Diagnostics* 2 (56), 3–18 (2011).
[4] I. G. Main, M.C. Forde, and J. Halliady, "Acoustic emission on bridges: experiments on concrete beams", *EWGAE 25th Eur. Conf. on Acoustic Emission Testing, Prague* I, I/127–I/134 (2002).
[5] L. Gołaski, G. Świt, M. Kalicka, and K. Ono, "Acoustic nondestructive techniques as a new method for evaluation of damages in prestressed concrete structures: failure of concrete structures", *J. Acoustic Emission* 24, 187–195 (2006).
[6] Ch. Grosse and F. Finck, "Quantitative evaluation of fracture processes in concrete using signal-based acoustic emission techniques", *Cement and Concrete Research* 28, 284–295 (2006)
[7] S. Granger, A. Loukili, G. Pijaudier-Cabot, and G. Chanvillard, "Experimental characterization of the self-healing of cracks in an ultra high performance cementitious material: mechanical test and acoustic emission analysis", *Cement and Concrete Research* 37, 519–527 (2007).
[8] J. Hoła, L. Sadowski, and K. Schabowicz, "Non-destructive identification of delamination in concrete floor toppingswith acoustic methods", *Automation in Construction* 20 (7), 799–807 (2011).
[9] G. Świt, *Predicting Failure Processes for Bridge – Type Structures Made of Prestressed Concrete Beams Using the Acoustic Emission Method*, Kielce University of Technology Kielce, Kielce, 2011, (in Polish).
[10] B. Goszczyńska, G. Świt, W. Trąmpczyński, A. Krampikowska, J. Tworzewska, and P. Tworzewski, "Experimental validation of concrete crack identification and location with the acoustic emission method", *Archives of Civil and Mechanical Engineering* 12 (1), 23–28 (2012).
[11] L.Gołaski, B. Goszczyńska, G. Świt, and W. Trąmpczyński, "System for the global monitoring and evaluation of damage processes developing within concrete structures under service loads", *The Baltic J. Road and Bridge Engineering* 7 (4), 237–245 (2012).
[12] Z. Ranachowski, "Application of acoustic emission to fault diagnosis in civil engineering", *Roads and Bridges* 2, 65–87 (2012), (in Polish).

[13] B. Goszczyńska, G. Świt, and W. Trąmpczyński, "Monitoring of active destructive processes as a diagnostic tool for the structure technical state evaluation", *Bull. Pol. Ac.: Tech.* 61, 97–108 (2013).

[14] B. Goszczyńska, "Analysis of the process of crack initiation and evolution in concrete with acoustic emission testing", *Archives of Civil and Mechanical Engineering* 14 (2), 134–143 (2014).

[15] T. Krykowski and A. Zybura, "Modeling of the environmental conditions effect on the reinforcement corrosion rate in concrete", *Cement Lime Concrete* 19 (3), 166-173 (2014).

[16] K. Nagrodzka-Godycka and P. Piotrkowski, "Experimental study of dapped-end beams subjected to inclined load", *ACI Structural J.* 1 (109), 11–20 (2012).

[17] B. Goszczyńska, W. Trąmpczyński, K. Bacharz, M. Bacharz, J. Tworzewska, and P. Tworzewski, "The experimental analysis of the spatial deformation of reinforced concrete beams with use of 3D optical scanner", *Engineering and Building* 3, 152–156 (2014), (in Polish).

[18] W. Kuczyński, *Concrete Structures. Continual Theory of Bending of Reinforced Concrete*, PWN, Warsaw, 1971, (in Polish).

[19] S. Goszczyński, *Theory of Continual Changes in Stiffness with Use of Stochastic Model of Reinforced Concrete*, Kielce University of Technology, Kielce, 1986, (in Polish).

[20] M. Iwański and A. Chomicz-Kowalska, "Laboratory study on mechanical parameters of foamed bitumen mixtures in the cold cycling technology", *11th Int. Conf. on Modern Building Materials, Structure and Techniques, Procedia Engineering* 57, 433–442 (2013).